

Synthesis of magnetite loaded fluorescence micelles of triblock copolymer

Bishnu Prasad Bastakoti ^{a,*}, John Bentley ^a, Destiny McLaurin ^a, Shin-ichi Yusa ^b, Surabhi Shaji ^c, Nikhil R. Mucha ^c, Dhananjay Kumar ^c, Tansir Ahamad ^d

^a Department of Chemistry, North Carolina Agricultural and Technical State University, 1601 E. Market St, Greensboro, NC 27411, USA

^b Department of Applied Chemistry, University of Hyogo, 2167 Shosha, Himeji, Hyogo 671-2280, Japan

^c Department of Mechanical Engineering, North Carolina Agricultural and Technical State University, 1601 E. Market St, Greensboro, NC 27411, USA

^d Department of Chemistry, College of Science, Bld#5, King Saud University, Riyadh, Saudi Arabia



ARTICLE INFO

Article history:

Received 23 January 2020

Accepted 25 February 2020

Available online 27 February 2020

Keywords:

Block copolymer

Micelle

Self-assembly

Magnetic nanoparticle

Nile red

Nano carrier

ABSTRACT

Magnetic micelles with fluorescence dyes were fabricated by self-assembly of triblock copolymer followed by in situ templated coprecipitation method. Nile red was encapsulated into the polystyrene core of the triblock copolymer confirmed by fluorescence measurement. The magnetic nanoparticles are selectively chemisorbed on the poly(acrylic acid) (PAA) shell of polymeric micelles due to ionic interaction between PAA and Fe ions. The negatively charged PAA also a platform to bind positively charged drug molecules. The hydrophilic poly(ethylene glycol) (PEG) corona stabilizes the micelles composites. The multifunctional polymeric micelles were well characterized by using different tools and techniques: dynamic light scattering, transmission electron microscope, UV-visible spectrophotometer, fluorescence spectroscope, and magnetometer.

Published by Elsevier B.V.

1. Introduction

The multifunctional nanosystems in therapeutics, which are simultaneously capable of diagnosis and treatment, hold great promise for the future of clinical treatment to enhance therapeutic efficacy [1–4]. Self-assembling polymeric micelles have long been explored for the development of multifunctional therapeutics due to their flexibility in properties such as reactivity, controlled composition, ability to encapsulate drug molecules and appropriate size [5]. Amphiphilic diblock and symmetric triblock copolymer (pluronics types; P123, F127) are widely studied block copolymer as nanocarriers for drugs and imaging agents together [6–12]. The amphiphilic block copolymer undergoes self-assembly and forms a hydrophobic core and hydrophilic shell. The hydrophobic drug molecules/imaging agents are protected within the hydrophobic core, while the hydrophilic shell can alter the pharmacokinetics and biodistribution of the incorporated drug through the interaction with biological environments [13]. Due to the ability of encapsulation of many hydrophobic drugs into its hydrophobic core, pluronics block copolymers has been widely employed in industrial formulations, particularly in pharmaceutical preparations. The poly(ethylene oxide) (PEO) corona can be functionalized with several hydrophilic molecules for targeting and imaging purpose in drug delivery [14]. Cholesterol grafted poly(*N*-

isopropylacrylamide-*co*-*N,N*-dimethylacrylamide-*co*-undecenoic acid) block copolymer forms a hydrophobic core that encapsulates hydrophobic drug paclitaxel and shell decorated with folate molecules for active tumor targeting. The polymer was designed in such a way that it showed the dual stimuli in drug delivery, that is, pH-induced thermosensitivity. The drug molecules released faster at pH 5 than at 7.4 [15].

In comparison to amphiphilic diblock and symmetric triblock copolymers, asymmetric triblock copolymers have attracted much attention because different morphologies have been observed for their micelles in the nanometer scale [16,17]. The introduction of the different third block offers additional parameters to control properties of the ABC-type block copolymers and then would afford interesting functionalities, thereby strongly influencing the self-assembly process [18–20]. Core-shell-corona micelles of the triblock copolymer has several advantages as a drug carrier. Armes and co-workers successfully loaded a model drug dipyridamole into the micelles of ABC triblock copolymer of methoxy-capped poly[ethylene glycol-*b*-2-(dimethyl amino)ethylmethacrylate-*b*-2-(diethylamino)ethyl methacrylate] by controlling the pH [21]. A triblock copolymer; poly(styrene-*b*-2-vinyl pyridine-*b*-ethylene oxide) (PS-*b*-PVP-*b*-PEO) with cationic shell in acidic condition was used as a carrier for the anionic drug coxicillin sodium. The drug was released significantly faster at physiological pH (7.4) compared to the acidic pH (3.0). Chemically reactive block not only provides the space for drug molecules but also a platform for the synthesis of inorganic based biomaterials [22,23]. Padwal et al.

* Corresponding author.

E-mail address: bpbastakoti@ncat.edu (B.P. Bastakoti).

synthesized polyacrylic acid stabilized magnetite nanoparticles. The composite nanoparticles along with anti-tuberculosis (TB) drug show the better efflux inhibitors to enhance the effectiveness of the drug in TB Treatment [24].

In this study, we use a laboratory synthesized triblock copolymer as a platform for imaging agents and drug molecules (Scheme 1). Poly(styrene-*b*-acrylic acid-*b*-ethylene oxides) (PS-*b*-PAA-*b*-PEG) block copolymer forms highly stable and robust micelles with polystyrene (PS) core, poly(acrylic acid) (PAA) shell and hydrophilic poly(ethylene glycol) (PEG) corona in water. The hydrophobic PS block encapsulates Nile red (optical imaging agent). The selective precipitation reaction of magnetic nanoparticles (magnetic imaging agent) occurs on anionic PAA shell. The composite micelles are stabilized by hydrophilic PEG corona. The binding of cationic drugs on anionic PAA block and their release were also studied. The core-shell-corona architecture of polymeric micelles can serve as a robust carrier for multiple payloads at a time. Moreover, the presence of frozen core and lower critical micelles' concentration, micelles are stable in a natural biological environment, even after dilution several times in the bloodstream could be the asset to be used as a drug carrier.

2. Experimental section

2.1. Materials

Poly(ethylene glycol) based macro-chain transfer agent (PEG₄₇-CTA, M_n (NMR) = 2360 g/mol) was prepared according to the reference [25]. 2,2'-Azobis(isobutyronitrile) (AIBN) was recrystallized from methanol. Acrylic acid (AA), 1,4-dioxane, and *N,N*-dimethylformamide were dried over 4 Å molecular sieves and distilled under reduced pressure. Tetrahydrofuran was dried over 4 Å molecular sieves and distilled. Styrene was washed with an aqueous alkaline solution and distilled from calcium hydride under reduced pressure. Water was purified with an ion-exchange system. Triblock copolymer (PS-*b*-PAA-*b*-PEG) composed of polystyrene (PS), poly(acrylic acid) (PAA), and poly(ethylene glycol) (PEG) (Scheme 2). The detail synthetic procedure is in supporting information. FeCl₃·6H₂O (Sigma Aldrich, 98%), FeCl₂·4H₂O (Sigma Aldrich, 99%), Nile red (NR, Sigma Aldrich, 99%), dibucaine hydrochloride (DC, Sigma Aldrich, 99%), phosphotungstic acid hydrate (Alfa Aesar), Tris buffer (Alfa Aesar) were used without purification.

2.2. Preparation of polymer solution

The polymer solution was prepared using a solvent exchange method. 0.1 g of polymer was dissolved into 10 mL of THF with mild sonication. The THF was exchanged with water by the dialysis method. In order to encapsulate NR into polymeric micelles, 1 mg NR and 0.1 g of polymer was dissolved in 10 mL of THF and the NR loaded micelles were

collected in water through dialysis. The dialysis was performed for 5 days against DI water. The water was changed 15 times, which ensures the complete replacement of THF with water. The solution was then transferred into a volumetric flask to obtain a stock solution with a concentration of 1 gL⁻¹ and the pH of the micelles' solution was maintained at 7.4 by using Tris-buffer. Magnetic nanoparticles were synthesized by the co-precipitation method [26]. 76 mg FeCl₃·6H₂O and 27 mg FeCl₂·4H₂O were dissolved in 20 mL polymer solution. A specific volume of ammonia solution was added into it. All reactions were carried out in N₂ protection.

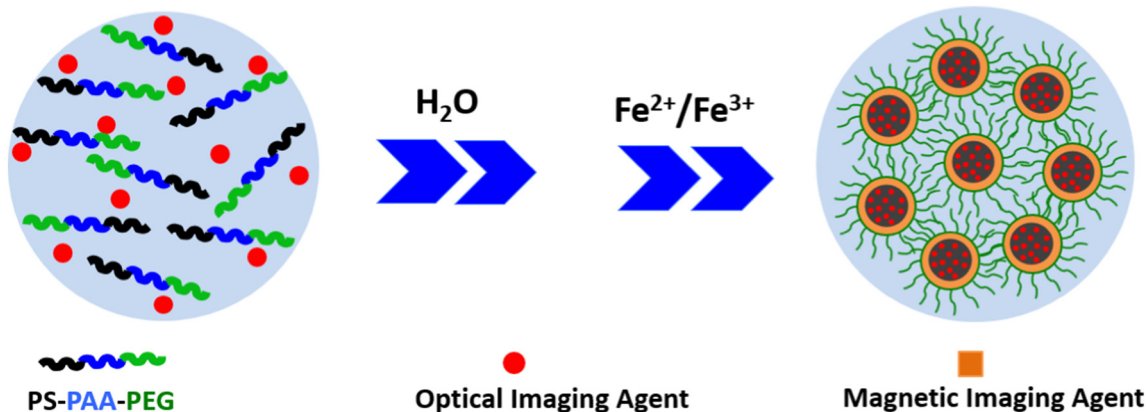
2.3. Characterization

Hydrodynamic diameter and zeta-potential were measured using an Otsuka ELS Z zeta-potential and particle analyzer. Transmission electron microscopy (TEM, JEM-2100F TEM) was used to see the polymeric micelles. The pure polymeric micelles were stained with phosphotungstic acid in order to improve the contrast. The polymer nanocomposites with magnetic nanoparticles were observed without the staining agent. The fluorescence spectra of NR were recorded by a fluorescence spectrophotometer (Jasco FP-6500) using right angle geometry, 1 cm × 1 cm quartz cells. The sample was excited at 488 nm in the measurement of fluorescence spectra, and the band widths were 3 and 1 nm on the excitation and emission sides, respectively. The drug release experiment was carried out in vitro using dialysis followed by UV-absorption measurements (Shimadzu-UV 2401PC). The drug loaded polymer nano complex solution was placed in a dialysis tube, and the amount of the drug released from the nano complexes was monitored at pH 7.4 maintained by a Tris buffer. 2.5 mL of the solution outside, then the dialysis tube was taken off at definite time intervals to measure the amount of dibucaine hydrochloride (DC) released. The solution after the UV absorption measurements was immediately returned to the bulk solution outside the dialysis tube to maintain the volume. The amount of the released DC was plotted versus the dialysis time.

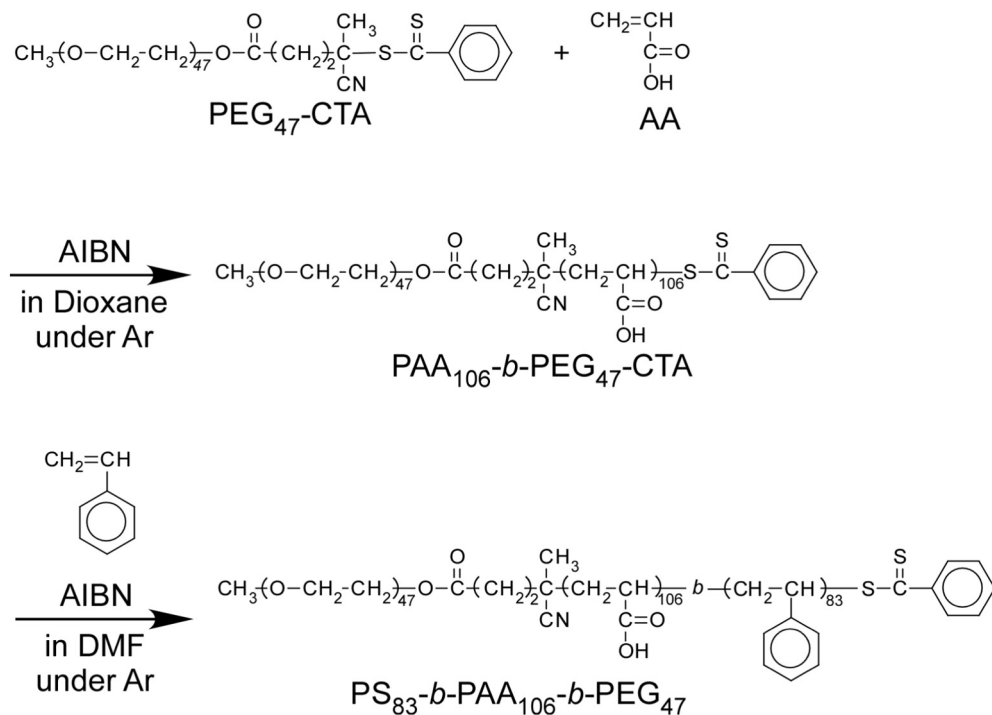
3. Results and discussion

3.1. Preparation of polymer solution and encapsulation of Nile red

PS₈₃-b-PAA₁₀₆-b-PEG₄₇ was synthesized via RAFT polymerization as reported previously [25]. The number in the parenthesis indicates the degree of polymerization of each block. The polymer was first dissolved in THF, a good solvent for all three blocks and the polymeric micelles were collected in water by the slow exchange of THF with water by dialysis method (Fig. 1). The polymer undergoes self-assembly in water and forms spherical micelles with PS core, PAA shell, and PEG corona. The hydrodynamic diameter of polymeric micelles depends on pH. The hydrodynamic diameter of the polymeric micelles was found to



Scheme 1. Fabrication of magnetite loaded fluorescence micelles of triblock copolymer.



Scheme 2. Synthetic route of PS-*b*-PAA-*b*-PEG via reversible addition-fragmentation chain transfer (RAFT) controlled radical polymerization.

be 52 nm to 72 nm depending on the pH of the solution. This change in hydrodynamic diameter (D_h) is due to conformation change in PAA block, PAA is a weak electrolyte with a carboxylic acid whose pK_a is 4.6 [27]. For $pH < pK_a$, most carboxylic groups exist as the protonated form (COOH), whereas for $pH > pK_a$, most carboxylic groups exist as the deprotonated form (COO^-) [28]. The deprotonated PAAs have more repulsion resulting in the larger hydrodynamic diameter. Fig. 2a shows the intensity-based DLS profile of PS-*b*-PAA-*b*-PEG at pH around 8. The distribution looks monodisperse which is also supported by a lower polydispersity index (0.09). The micelles are dried and observed under a TEM. The TEM measurements provided concrete evidence for the formation of the spherical micelles. The polymeric micelles are stained with the dilute phosphotungstic acid solution in order to improve the contrast. The white sphere of around 25 nm average diameter in the TEM photograph (Fig. 3a) corresponds to the hard PS core because the phosphotungstic acid preferentially stains the PS core. The size of micelles from TEM is smaller than the size measured from DLS. The size discrepancy between the DLS and TEM measurements is due

to the different sample preparation methods. The DLS measurements were carried out in solution and the TEM measurements were made on a dry sample under high vacuum.

The polymeric micelles of the amphiphilic block copolymer are widely used as a platform for encapsulation of photo responsive molecules which have wide applications in imaging and delivery of hydrophobic drug molecules. Different from previously reported encapsulation methods [29,30], the complicated chemical conjugation of the dyes with polymer micelles is avoided here. NR is a hydrophobic imaging dye which exhibits high quantum yield in nonpolar environments. However, in polar environments such as water, the quantum yield approaches zero [31]. These spectral features of NR have led to a wide range of applications such as evaluation of lipids, and contrast agent in radiometric imaging [32]. The hydrophobic NR with photo bleaching properties in polar solvents provides an additional tool for the evaluation of potential interactions between the encapsulated dye and the surrounding solvent. Polymers and NR were first dissolved in THF. Slowly exchanging THF with water, the NR was encapsulated selectively into PS core due to hydrophobic interactions. NR is poorly soluble in water and does not emit fluorescence in a polar environment. Encapsulation and micellization occur simultaneously as shown in Scheme 1. NR is well protected inside the polymeric micelles more specifically into the PS core. The very clear and stable emission spectrum of NR in aqueous micelles' solution was obtained (Fig. 4). NR is a benzophenoxazone dye and uncharged hydrophilic molecule which do not show its fluorescence properties in a polar solvent such as water. Since the fluorescence intensity did not change for several days confirm that NR is tightly intact into the PS core (data not shown). The encapsulation of NR into micelles does not significantly change the hydrodynamic diameter and surface charge of polymeric micelles.

3.2. Magnetic properties

Magnetic nanoparticles have been extensively studied for a range of biomedical applications including magnetic resonance imaging (MRI), drug delivery and hyperthermia [33]. The amphiphilic block copolymer is particularly promising tools due to their chemical diversity, stability controllable molecular weight. Generally, pre-

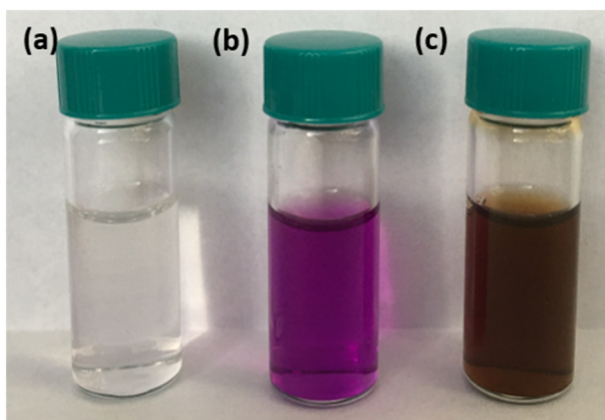


Fig. 1. Photographs of (a) pure micelles, (b) Nile red loaded micelles and (c) magneto micelles.

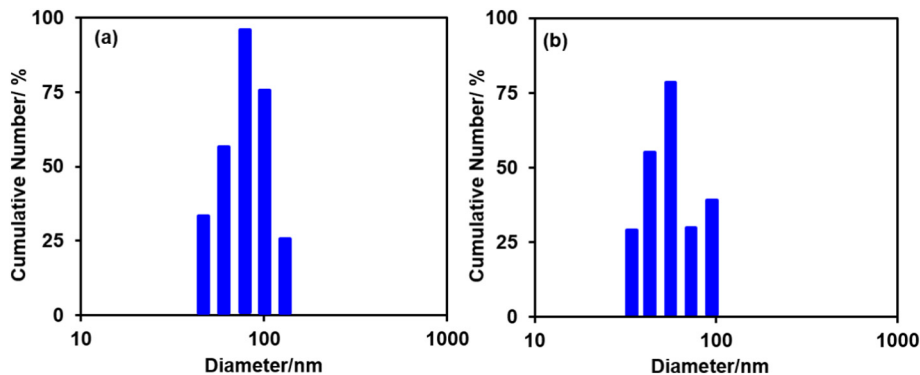


Fig. 2. Hydrodynamic diameter of (a) PS-*b*-PAA-*b*-PEG micelles and (b) Fe ions/PS-*b*-PAA-*b*-PEG micelles composite.

synthesized hydrophobic magnetic nanoparticles were encapsulated into the nanocarriers [34]. Here, we used a conventional in-situ synthesis method of Fe_3O_4 nanoparticles via coprecipitation of ferric and ferrous salts in alkaline media. The PS-*b*-PAA-*b*-PEG polymeric micelles are used as a platform to synthesize magnetic nanoparticles. A mixture of iron (II) and iron (III) salts was allowed to interact with PS-*b*-PAA-*b*-PEG polymeric micelles. Fe^{2+} and Fe^{3+} ions first interact with PAA segments electrostatically. Iron ion's complexation occurred with the carboxylic acid groups from the PAA segments via intramolecular and/or intermolecular complexation [35]. As a result of the interaction, the zeta-potential was increased to -8 mV from -32 mV. Whereas, the hydrodynamic diameter decreases from 72 nm to 55 nm (Fig. 2b). Due to the presence of free PEO, the composite particles were stable even the zeta potential close to zero. The chelating complex was then precipitated by the dropwise addition of ammonia solution to yield iron oxide nanoparticles. The solution was stirred for 30 min in an N_2 environment at 80 °C. The hydrodynamic diameter of polymer/magnetic nanoparticle composites was found to be 295 nm with significantly higher polydispersity index (0.3). This is due to the formation of secondary nano/micro aggregates. TEM measurements were performed to observe the effects of iron oxide formation on the triblock copolymer micelles (Fig. 3b). The dark shell of polymeric micelles with ultra-small dots iron oxide confirmed the formation of iron oxides.

Shown in Fig. 5a are the zero field cooled (ZFC) and field cooled (FC) magnetization plots for Fe_3O_4 nanoparticles as a function of temperature at 0.02 , 0.05 , and 0.1 T. In the ZFC magnetization measurements, the sample is first cooled to 10 K in zero field and then a magnetic field is applied. The magnetization data is recorded

while warming up the sample with temperature being stabilized at each step. In the FC cooled magnetization measurements, the sample is cooled in the presence of the same magnetic field which is used during the ZFC measurements and then the magnetization data is recorded while warming up the sample. A few things are worthy of a note from these plots. First, both ZFC and FC magnetization increases as the values of a field applied increase. Secondly, all three ZFC curves have a maximum in magnetization that is function of field applied, viz. 120 K at 0.02 T, 80 K at 0.05 T, and 60 K at 0.1 T. The temperature at which the maximum in magnetization occurs is known as blocking temperature for superparamagnetic particles. Third, FC magnetization increases monotonically as the temperature decreases for all the three fields. Besides, there is a bifurcation in ZFC and FC curves that is dependent on the field applied. For example, the bifurcation temperature is 140 K and 80 K at 0.02 , 0.05 T respectively. The ZFC-FC bifurcation temperature is also considered at the blocking temperature. Ideally, the ZFC maximum and bifurcation temperature should match with each other. While these temperatures are identical for 0.05 T, there is a small deviation in the peak and bifurcation temperature (~ 20 K). This deviation in the ZFC maximum and bifurcation temperature is attributed to the distribution in a particle size in the sample as noted in Fig. 5a.

The magnetization versus field plots for coprecipitated Fe_3O_4 nanoparticles are shown in Fig. 5b. While the sample has a distinct opening in the magnetic hysteresis (MH) loop at 10 K with a value of coercivity ~ 350 Oe, the MH loops are almost close with no appreciable coercively at 100 , 200 and 300 K. This suggests that the sample is superparamagnetic above 100 K. The signature of super paramagnetism in our sample is obtained by plotting magnetization as a function of H/T

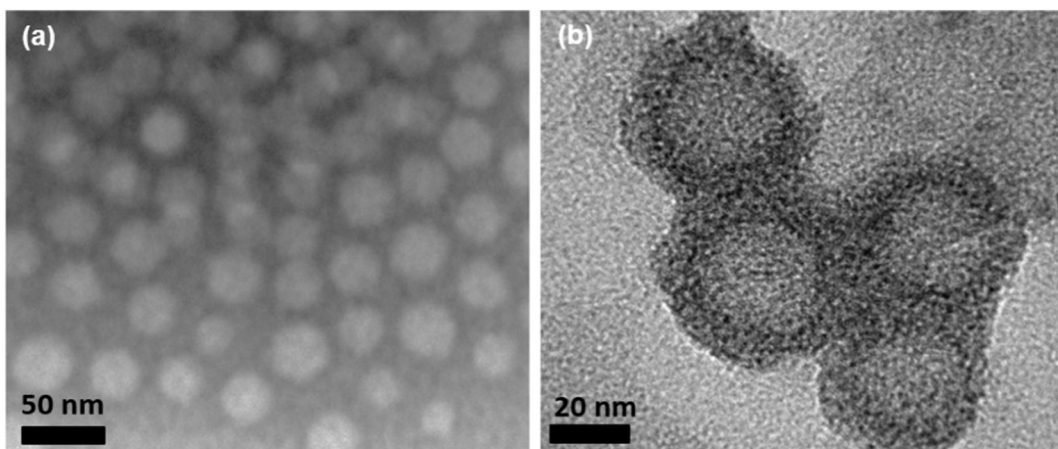


Fig. 3. TEM images of (a) polymeric micelles and (b) magneto micelles.

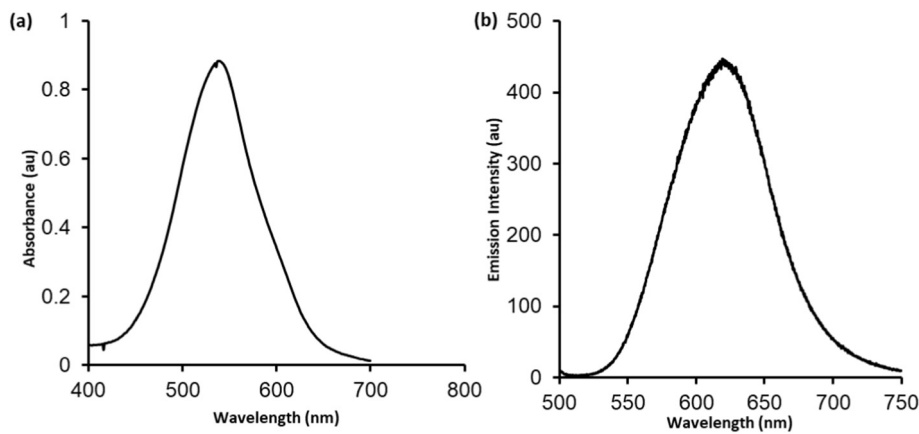


Fig. 4. Absorption and emission spectra of Nile red in the polymer solution.

in the inset of Fig. 5b. The collapsing of the MH loops at 100, 200, and 300 K in the inset figure confirms the superparamagnetic behavior of coprecipitated Fe_3O_4 particles.

3.3. Interaction of dibucaine with polymeric micelles and its release

Dibucaine hydrochloride (DC) is a positively charged anesthetic agent and a model drug in the present study. It is interesting to incorporate positively charged drug molecules DC into the negatively charged polymeric micelles. The DC and polymer is mixed in such a way that the PAA and DC molar ratio is 1:1. The hydrodynamic diameter of polymeric micelles decreases from 72 nm to 58 nm after loading the DC. The decrease in the diameter is attributed to the neutralization of the anionic acrylic acid ion of the PAA block by positively charged DC. The neutralization masks the negative charge of PAA which weakens the repulsion among the PAA blocks. It is also confirmed by measuring zeta potential measurements. The surface charges of polymeric micelles increase to +3 mv from -32 mv in polymer-DC nanocomposites. The drug-loaded micelles were stable in aqueous solutions, exhibiting no aggregation or precipitation. The dimension of the drug-loaded micelles (58 nm) is suitable for a drug carrier because this size prevents elimination via either renal excretion or mechanical filtration by inter-endothelial cell-slits in the spleen [36]. In this system, each block of the polymer exhibits its unique function. The hydrophobic core prevents the micelles from collapse even in an extremely diluted condition in biological environments. The anionic PAA shell works as a binding site for cationic drugs. Compared with the covalently bonded drug, the electrostatic interaction is easy to control the drug release. The PEG corona stabilizes the nano complexes to prevent aggregation because of its high hydration level and steric repulsion between the chains. The

in vitro drug release from DC/PS-PAA-PEG micelles was performed using a dialysis method at room temperature, the pH of the release media was maintained at 7.4 by using tris buffer (Fig. 6). The amount of released drug was monitored at the outside of the dialysis membrane. The absorbance of DC was recorded at 226 nm. It was observed that the drugs were released sustainably without burst release.

4. Conclusion

We have successfully used laboratory synthesized triblock copolymer to encapsulate hydrophobic molecules into core of micelles and superparamagnetic Fe_3O_4 nanoparticles on the shell of micelles which have already encapsulated Nile red in the core. The synthetic method is simple, and a complex chemical conjugation between organic molecules and polymer is unnecessary. The strong chelating behavior of PAA shell provides the reaction sites for iron ions and controls the crystal overgrowth during co-precipitation reaction. The strong binding between cationic drugs and polymeric micelles was confirmed by dynamic light scattering experiment and it was found that the drug is mainly released by the diffusion mechanism. We believe that the encapsulation of fluorescent molecules and controlled deposition of nanoparticles with superparamagnetic properties into the shell of self-assembled polymeric micelles will lead to fabrication of multifunctional nanoparticles.

Declaration of competing interest

The authors declare that they have no known competing financial interests or personal relationships that could have appeared to influence the work reported in this paper.

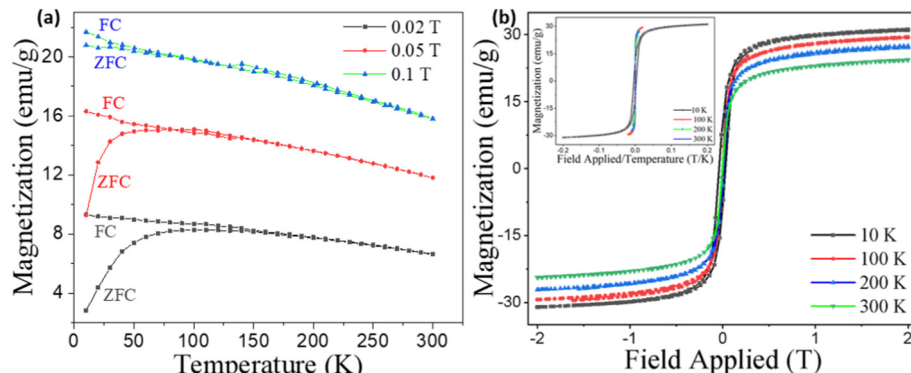


Fig. 5. ZFC and FC magnetization as a function of temperature at 0.02, 0.05 and 0.1 T. (b) Magnetization as a function of field applied at 10, 100, 200, and 300 K. The inset confirms the superparamagnetic behavior of Fe_3O_4 particles.

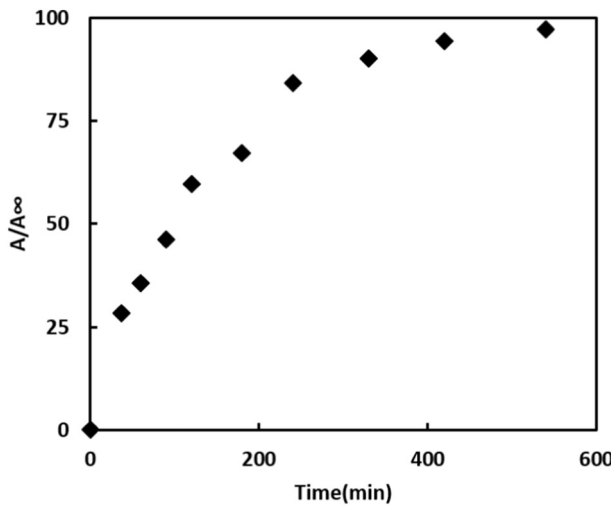


Fig. 6. Drug release profile of dibucaine from polymeric micelles.

Acknowledgements

The authors thank the researchers supporting project number (RSP-2019/6), King Saud University, Riyadh, Saudi Arabia. Part of the work was performed at the Joint School of Nanoscience and Nanoengineering, a member of Southeastern Nanotechnology Infrastructure Corridor (SENIC) and National Nanotechnology Coordinated Infrastructure (NNCI), which is supported by the National Science Foundation (ECCS-1542174).

Appendix A. Supplementary data

Supplementary data (the detail synthesis and characterization of block copolymer) to this article can be found online at <https://doi.org/10.1016/j.molliq.2020.112785>.

References

- [1] M. Fathi, J. Barar, Perspective highlights on biodegradable polymeric nanosystems for targeted therapy of solid tumors, *Bioimpacts* 7 (1) (2017) 49–57.
- [2] H.L. Sun, Y.F. Zhang, Z.Y. Zhong, Reduction-sensitive polymeric nanomedicines: an emerging multifunctional platform for targeted cancer therapy, *Adv Drug Deliver Rev* 132 (2018) 16–32.
- [3] H. Yang, C.C. Zhang, T.T. Li, X. Shen, Z.Y. Chen, X.X. Xie, S. Li, X. Qin, C.H. Wu, Y.Y. Liu, Rational design of multifunctional polymeric micelles with stimuli-responsive for imaging-guided combination cancer therapy, *J. Biomed. Nanotechnol.* 13 (10) (2017) 1221–1234.
- [4] T.Y. Lin, Y.P. Li, H.Y. Zhang, J.T. Luo, N. Goodwin, T.J. Gao, R.D. White, K.S. Lam, C.X. Pan, Tumor-targeting multifunctional micelles for imaging and chemotherapy of advanced bladder cancer, *Nanomedicine-Uk* 8 (8) (2013) 1239–1251.
- [5] K. Kataoka, A. Harada, Y. Nagasaki, Block copolymer micelles for drug delivery: design, characterization and biological significance, *Adv Drug Deliver Rev* 64 (2012) 37–48.
- [6] A. Pitt-Barry, N.P.E. Barry, Pluronic (R) block-copolymers in medicine: from chemical and biological versatility to rationalisation and clinical advances, *Polym Chem-Uk* 5 (10) (2014) 3291–3297.
- [7] Y. Xu, Y.Y. Lu, L. Wang, W. Lu, J. Huang, B. Muir, J.H. Yu, Nanomicelles based on a boronate ester-linked diblock copolymer as the carrier of doxorubicin with enhanced cellular uptake, *Colloid Surface B* 141 (2016) 318–326.
- [8] H. Hyun, Y.H. Kim, I.B. Song, J.W. Lee, M.S. Kim, G. Khang, K. Park, H.B. Lee, In vitro and in vivo release of albumin using a biodegradable MPEG-PCL diblock copolymer as an in situ gel-forming carrier, *Biomacromolecules* 8 (4) (2007) 1093–1100.
- [9] K. Osada, H. Cabral, Y. Mochida, S. Lee, K. Nagata, T. Matsuurra, M. Yamamoto, Y. Anraku, A. Kishimura, N. Nishiyama, K. Kataoka, Bioactive polymeric metalloosomes self-assembled through block copolymer-metal complexation, *J. Am. Chem. Soc.* 134 (32) (2012) 13172–13175.
- [10] V. Torchilin, Multifunctional and stimuli-sensitive pharmaceutical nanocarriers, *Eur. J. Pharm. Biopharm.* 71 (3) (2009) 431–444.
- [11] C.F. Lee, C.H. Yang, T.L. Lin, P. Bahadur, L.J. Chen, Role of molecular weight and hydrophobicity of amphiphilic tri-block copolymers in temperature-dependent co-micellization process and drug solubility, *Colloid Surface B* 183 (2019).
- [12] A. Raval, S.A. Pillai, A. Bahadur, P. Bahadur, Systematic characterization of Pluronic micelles and their application for solubilization and in vitro release of some hydrophobic anticancer drugs, *J. Mol. Liq.* 230 (2017) 473–481.
- [13] Y.Y. He, Y. Zhang, Y. Xiao, M.D. Lang, Dual-response nanocarrier based on graft copolymers with hydrazone bond linkages for improved drug delivery, *Colloid Surface B* 80 (2) (2010) 145–154.
- [14] L.W. Liu, K.T. Yong, I. Roy, W.C. Law, L. Ye, J.W. Liu, J. Liu, R. Kumar, X.H. Zhang, P.N. Prasad, Bioconjugated pluronic triblock-copolymer micelle-encapsulated quantum dots for targeted imaging of cancer: in vitro and in vivo studies, *Theranostics* 2 (7) (2012) 705–713.
- [15] W.Y. Seow, J.M. Xue, Y.Y. Yang, Targeted and intracellular delivery of paclitaxel using multi-functional polymeric micelles, *Biomaterials* 28 (9) (2007) 1730–1740.
- [16] R. Wang, P. Tang, F. Qiu, Y.L. Yang, Aggregate morphologies of amphiphilic ABC tri-block copolymer in dilute solution using self-consistent field theory, *J. Phys. Chem. B* 109 (36) (2005) 17120–17127.
- [17] T.I. Lobling, O. Borisov, J.S. Haataja, O. Ikkala, A.H. Groschel, A.H.E. Muller, Rational design of ABC triblock terpolymer solution nanostructures with controlled patch morphology, *Nat. Commun.* 7 (2016).
- [18] B.P. Bastakoti, Y.Q. Li, T. Kimura, Y. Yamauchi, Asymmetric block copolymers for supramolecular templating of inorganic nanospace materials, *Small* 11 (17) (2015) 1992–2002.
- [19] C.A. Fustin, V. Abetz, J.F. Gohy, Triblock terpolymer micelles: a personal outlook, *Eur. Phys. J. E* 16 (3) (2005) 291–302.
- [20] B.P. Bastakoti, S. Ishihara, S.Y. Leo, K. Ariga, K.C.W. Wu, Y. Yamauchi, Polymeric micelle assembly for preparation of large-sized mesoporous metal oxides with various compositions, *Langmuir* 30 (2) (2014) 651–659.
- [21] Y.Q. Tang, S.Y. Liu, S.P. Armes, N.C. Billingham, Solubilization and controlled release of a hydrophobic drug using novel micelle-forming ABC tri-block copolymers, *Biomacromolecules* 4 (6) (2003) 1636–1645.
- [22] B.P. Bastakoti, S. Guragain, Y. Yokoyama, S. Yusa, K. Nakashima, Synthesis of hollow CaCO_3 nanospheres templated by micelles of poly(styrene-b-acrylic acid-b-ethylene glycol) in aqueous solutions, *Langmuir* 27 (1) (2011) 379–384.
- [23] M. Sasisudhan, H.N. Luitel, N. Gunawardhana, M. Inoue, S. Yusa, T. Watari, K. Nakashima, Synthesis of magnetic $\alpha\text{-Fe}_2\text{O}_3$ and Fe_3O_4 hollow nanospheres for sustained release of ibuprofen, *Mater. Lett.* 73 (2012) 4–7.
- [24] P. Padwal, R. Bandyopadhyaya, S. Mehra, Polyacrylic acid-coated iron oxide nanoparticles for targeting drug resistance in mycobacteria, *Langmuir* 30 (50) (2014) 15266–15276.
- [25] S. Yusa, Y. Yokoyama, Y. Morishima, Synthesis of oppositely charged block copolymers of poly(ethylene glycol) via reversible addition-fragmentation chain transfer radical polymerization and characterization of their polyion complex micelles in water, *Macromolecules* 42 (1) (2009) 376–383.
- [26] P.P. Li, J.L. Huang, Preparation of poly(ethylene oxide)-graft-poly(acrylic acid) copolymer stabilized iron oxide nanoparticles via an in situ templated process, *J. Appl. Polym. Sci.* 109 (1) (2008) 501–507.
- [27] S.W. Cranford, C. Ortiz, M.J. Buehler, Mechanomutable properties of a PAA/PAH polyelectrolyte complex: rate dependence and ionization effects on tunable adhesion strength, *Soft Matter* 6 (17) (2010) 4175–4188.
- [28] B.P. Bastakoti, S. Guragain, K. Nakashima, Y. Yamauchi, Stimuli-induced core-corona inversion of micelle of poly(acrylic acid)-block-poly(*N*-isopropylacrylamide) and its application in drug delivery, *Macromol. Chem. Phys.* 216 (3) (2015) 287–291.
- [29] C. Elvira, A. Gallardo, J. San Roman, A. Cifuentes, Covalent polymer-drug conjugates, *Molecules* 10 (1) (2005) 114–125.
- [30] H. Park, Y.J. Jin, G. Kwak, Combination of a fluorescent conjugated polymer, photochromic dye, and UV-curable acryl oligomer for fluorescence switching applications, *Dyes Pigments* 146 (2017) 398–401.
- [31] V. Martinez, M. Henary, Nile red and Nile blue: applications and syntheses of structural analogues, *Chem-Eur J* 22 (39) (2016) 13764–13782.
- [32] J.R. Korber, C.W. Barth, S.L. Gibbs, Nile red derivatives enable improved ratiometric imaging for nerve-specific contrast, *J. Biomed. Opt.* 23 (7) (2018).
- [33] X.M. Li, J.R. Wei, K.E. Aifantis, Y.B. Fan, Q.L. Feng, F.Z. Cui, F. Watari, Current investigations into magnetic nanoparticles for biomedical applications, *J. Biomed. Mater. Res. A* 104 (5) (2016) 1285–1296.
- [34] R.J. Hickey, A.S. Haynes, J.M. Kikkawa, S.J. Park, Controlling the self-assembly structure of magnetic nanoparticles and amphiphilic block-copolymers: from micelles to vesicles, *J. Am. Chem. Soc.* 133 (5) (2011) 1517–1525.
- [35] S.E. Kudaibergenov, N. Nuraje, Intra- and interpolyelectrolyte complexes of polyampholytes, *Polymers-Basel* 10 (10) (2018).
- [36] V.P. Torchilin, Structure and design of polymeric surfactant-based drug delivery systems, *J. Control. Release* 73 (2–3) (2001) 137–172.